Spontaneous structure formation in a network of dynamic elements

Junji Ito
Laboratory for Perceptual Dynamics, Brain Science Institute, RIKEN, 2-1, Hirosawa, Wako-shi, Saitama 351-0198, Japan

Kunihiko Kaneko
Department of Pure and Applied Sciences, University of Tokyo, Komaba, Meguro-ku, Tokyo 153-8902, Japan
(Received 17 December 2002; published 29 April 2003)

To discover the generic behaviors of dynamic networks, we study a coupled map system with variable coupling strength. It is found that this system spontaneously forms various types of network structure according to the parameter values. Depending on the synchronized or desynchronized motion of unit dynamics, the network structure can be either static or dynamic. The separation of units into two groups, one composed of units with a large number of outgoing connections and the other units with little outgoing connections, is observed in dynamic structure. It is revealed that the mechanism for such separation is a positive feedback between unit and connection dynamics.

DOI: 10.1103/PhysRevE.67.046226 PACS number(s): 89.75.Fb

I. INTRODUCTION

Complex networks appear in a variety of systems such as metabolic networks [1], neural networks [2], ecological networks [3,4], collaboration networks [4], sexual networks [5], the worldwide web [6], and so forth. Recent studies on these complex networks have revealed some generic features observed commonly in a wide range of natural and artificial networks [7].

Most of these studies are inspired mainly by two works concerning the structure of networks: one is the study of the small world effect by Watts and Strogatz [8], and the other is the scale-free property by Barabási and Albert [9]. Due to the structural interest in these original studies, the following works also focus on the structure of networks, unduly ignoring the dynamics of network elements.

However, the elements in most realistic networks have their own dynamics, and their dynamics have an influence on the formation of the network structure. Here the dynamics of each element and the dynamics of the network structure are mutually related. Such interplay between these two dynamics seems to play a crucial role, especially in the functioning of living and social systems.

By the term dynamic network, we refer to networks whose structure evolves in time in relation with the dynamics of elements. The aim of the present paper is to discover the generic behaviors of the dynamic networks and to reveal the mechanism of their occurrence, by constructing a simple model of a dynamic network and analyzing its behavior computationally.

To capture the generic properties of dynamic networks, our model should be simple enough to possess only generic features observed in a variety of dynamic networks. Here we adopt a coupled map with variable coupling strength [10] as our model because of its simplicity and ability to reproduce generic behaviors observed in high-dimensional (chaotic) dynamical systems [11].

After introducing our model in the following section, we describe the basic properties of the model in Sec. III. The behaviors are classified into several phases. From Sec. IV to Sec. VI, we focus only on one specific phase, namely, desynchronized phase, where the structure of the network changes dynamically in relation with unit dynamics. In Sec. IV, we define two quantitative measures which reflect the dynamic properties of network structures and classify the type of the networks observed in our model utilizing these measures. In Sec. V, the structural properties of each type of network are studied. In Sec. VI, we reveal the mechanism of structure formation in our network. A summary of the results and discussion are given in Sec. VII.

II. MODEL

As mentioned above, we adopt a coupled map system as our model. Let f be the map that governs the dynamics of each unit in the network, and x_n^i be the state variable of the ith unit, where the index n represents the time step. Additionally, let w_n^{ij} be the time dependent strength of the connection from unit j to unit i at the nth step. Then, the dynamics of unit i are described by the following equation:

$$x_{n+1}^i = (1-c) f(x_n^i) + c \sum_j^N w^{ij} f(x_n^j),$$

where c is the parameter that represents the strength of the interaction from other units to the unit i, and N is the number of units in the system. We use the logistic map $f(x)=ax(1-x)$ in the present paper, since it is thoroughly investigated as a simple model showing periodic dynamics with any period as well as chaos.

The above model belongs to the class of models called globally coupled map (GCM) [12]. The GCM model with a constant coupling strength $w^{ij}=1/N$, taking identical values for all (i,j), has been studied extensively and intensively [13]. The above model is an extension of the GCM to allow for the change of the coupling strength.

We impose two restrictions on the dynamics of connection strength w_n^{ij}. First, connections between units whose state variables have similar values are strengthened. This is an extension of Hebb's rule to a system with continuous state

variables. Second, the total weight of connections conversing on a single unit is normalized to be unity. This choice is natural, since in any network some limitation is imposed on the resource to establish and maintain connections between units. The competition among connection strengths is inevitable under such a limitation. If there is competition for the coupling strength among the connections coming into a given element, the above form of normalization of connection strength gives a simple expression of such competition. This choice is also convenient to avoid the divergence of connection strength between synchronized units. We adopt one of the simplest equations which satisfies the above two restrictions, given as follows:

$$w_{n+1}^{ij}=\frac{[1+\delta g(x_n^i,x_n^j)]w_n^{ij}}{\sum_{j=1}^{N}[1+\delta g(x_n^i,x_n^j)]w_n^{ij}},$$

where the parameter δ represents the degree of plasticity of the connection and takes a value from 0 to 1. We use $\delta=0.1$ throughout this paper for simplicity. Dependence of the system's behavior on δ will be discussed later. g is a monotonically decreasing function of the difference between its two arguments. We use $g(x,y)=1-2|x-y|$ in the present paper, to assure this monotonicity, but other forms with this nature yield the same result.

To sum up, our model is described by the following set of equations:

$$x_{n+1}^i=f\left((1-c)x_n^i+c\sum_{j=1}^{N}w_n^{ij}x_n^j\right),$$

$$f(x)=ax(1-x),$$

$$w_{n+1}^{ij}=\frac{[1+\delta g(x_n^i,x_n^j)]w_n^{ij}}{\sum_{j=1}^{N}[1+\delta g(x_n^i,x_n^j)]w_n^{ij}},$$

$$g(x,y)=1-2|x-y|.$$

For most numerical simulations shown below, we choose the following initial condition. First, the initial value of self-connection w_0^{ii} is set to 0. Hence, the self-connections are kept at 0 at any time step n. Second, all the remaining connection strengths are set to be identical. This means that initially every unit in the system uniformly connects with all the other units. From the constraint of the normalization, the initial connection strength is determined to be $1/(N-1)$. Finally, x_0^i is randomly chosen from the uniform distribution between 0 and 1.

III. BASIC PROPERTIES OF THE MODEL

We start our analysis by studying the dependence of the system's behavior on the values of the parameters a and c. According to Ref. [12], the dynamics of globally coupled maps are generally classified into four phases, i.e., coherent phase, ordered phase, partially ordered phase, and desynchronized phase. Differently from the conventional GCM, where the connection strengths are fixed, the partially ordered phase does not appear in our model [17]. The phase diagram of our model against parameters a and c is shown in Fig. 1.

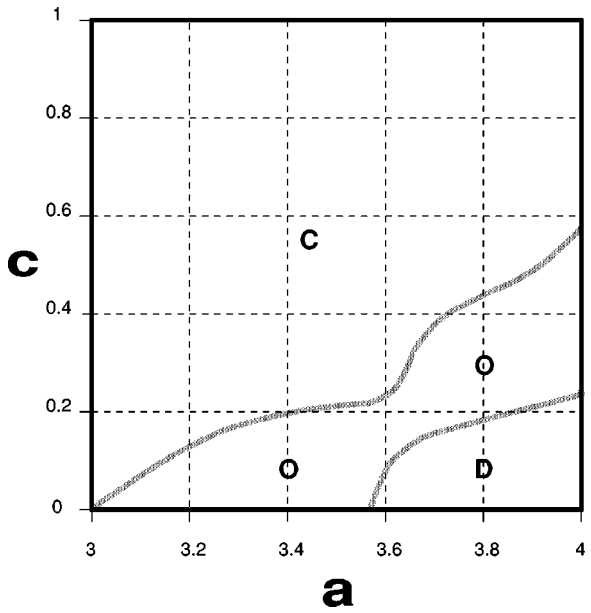

FIG. 1. Rough phase diagram of the model against the parameters a and c, obtained by computing the number of clusters. The simulation is carried out by changing both of the parameter values by 0.01. Letters in the figure represent the following: *C*, coherent phase; *O*, ordered phase; *D*, desynchronized phase.

The behavior for each set of the parameters is almost independent of the initial conditions. Aside from the initial condition mentioned above, we have also carried out the simulation starting from random initial configurations for connection strengths. From these simulations, the phase diagram shown in Fig. 1 (using the homogeneous initial connection strengths) is reproduced, although the boundaries between phases are slightly shifted.

In the rest of this section, we briefly describe the dynamical properties of units and connections in each phase.

A. Coherent phase

In the coherent phase, all units oscillate synchronously. Since, in our system, the change of the connection strength is proportional to the difference between units' state variables, the connection strengths do not change in a synchronized state. Before all the units synchronize, the connection strength changes in the transient. However, the convergence to the synchronized state is so rapid that the connection change during the transient period is quite small. Hence, in the coherent phase, the network structure is static and all the connection strengths are almost the same as the initial values. In Fig. 2, the connection matrix in the coherent phase is illustrated.

The stability of the synchronized state can be easily computed by the following condition for the split exponent (tan-

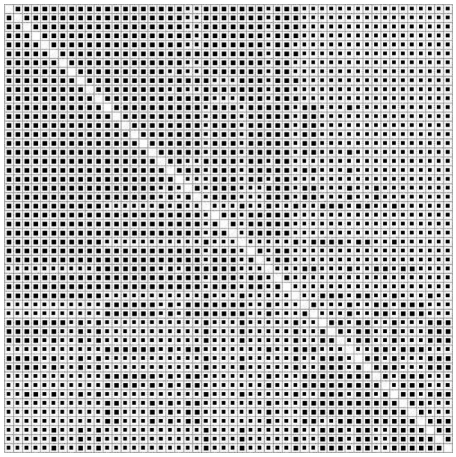

FIG. 2. Connection matrix w^{ij} in the coherent phase. The value of w^{ij} is represented by the size of the filled square at the ith row, jth column. The scale is chosen so that the size of the corresponding square is half of the grid size when $w^{ij}=1/(N-1)$. $N=50$, $a=3.6$, $c=0.3$.

gential Lyapunov exponent) [12]:

$$\lambda_{\mathrm{spl}}=\ln\left(1-\frac{N}{N-1}c\right)+\lim_{T\to\infty}\frac{1}{T}\sum_{n=1}^{T}\ln|f'(x_n^i)|<0.$$

Since the dynamics of the connection strength are driven by the difference between the state variables, the network structure is also stable if the synchronized state is stable. Hence, the stability of the network structure is also evaluated by the above condition.

B. Ordered phase

In the ordered phase, units spontaneously form several clusters, within which units oscillate synchronously. The connection strengths between the units in the same cluster are almost the same, while the connection between units in different clusters vanishes to zero. The connection strength within a cluster is given by about $1/N_c$, due to the normalization condition.

The number of the clusters is 2 near the boundary against the coherent phase [see Fig. 3 (top)], and the number increases as the parameter a increases or the parameter c decreases. The maximum number of the clusters is $N/2$, which is taken near the boundary against the desynchronized phase. In this $N/2$-cluster state, every two units form a pair and they have connection only between each other. In Fig. 3 (bottom), the connection matrix of the $N/2$-cluster state is shown.

The stability of a cluster can be evaluated again by the split exponent. The split exponent of a cluster of N_{c} units is

$$\lambda_{\mathrm{spl}}=\ln|1-(1+w^{ij})c|+\lim_{T\to\infty}\frac{1}{T}\sum_{n=1}^{T}\ln|f'(x_n^i)|.$$

The second term the equals Lyapunov exponent for the map $x'=f(x)$. Since, as mentioned above, $w^{ij}\sim 1/(N_c-1)$ within the cluster, we can get the following expression of the split exponent

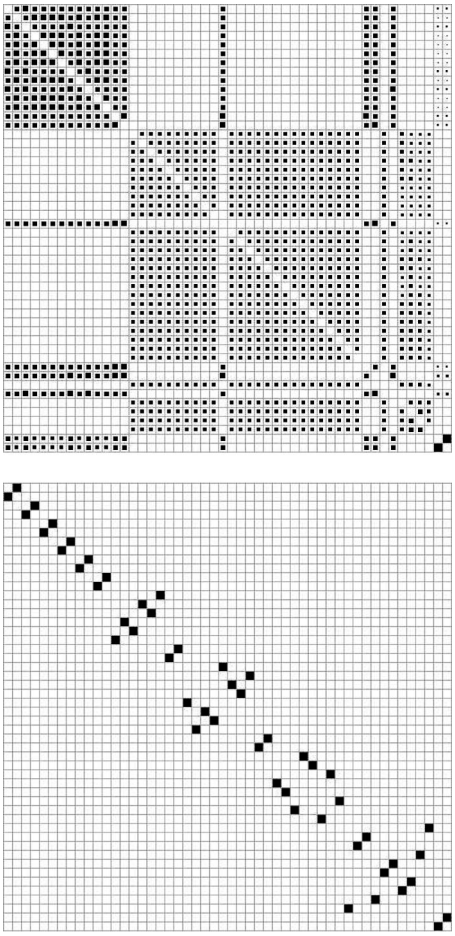

FIG. 3. Connection matrices w^{ij} in the ordered phase, displayed with the same procedure as in Fig. 2. $N=50$. (Top) Connection matrix of the two-cluster state. The scale is chosen so that the size of the corresponding square is half of the grid size when $w^{ij}=1/(N/2-1)$. $a=3.6$, $c=0.2$. (Bottom) Connection matrix of the $N/2$-cluster state. The scale is chosen so that the size of the corresponding square is the same as the grid size $w^{ij}=1$. $a=3.97$, $c=0.3$.

$$\lambda_{\mathrm{spl}}\sim\ln\left|1-\left[1+\frac{1}{(N_{\mathrm{c}}-1)}\right]c\right|+\lambda_0,$$

where λ_0 is the Lyapunov exponent of $f(x)$. Note that the stability of a cluster depends on the size of the cluster N_{c}.

Especially, for the $N/2$-cluster state, the split exponent can be written as

$$\lambda_{\mathrm{spl}}=\ln|1-2c|+\lambda_0.$$

The boundary between the ordered phase and the desynchronized phase is determined by the equation $\ln|1-2c|+\lambda_0=0$.

C. Desynchronized phase

In the desynchronized phase, there is no synchronization between any pair of units. Unlike the coherent and the ordered phases, the difference between state variables is finite and changes in time. Accordingly, the connection strengths also vary in time and the network forms a complex structure

with temporal evolution in this phase. Depending on the parameter values, our model shows three different types of network structure.

The structure of the first type is similar to the $N/2$-cluster state. In this phase, however, differently from the ordered phase, the dynamics of the units forming a pair are not synchronized, although they are strongly correlated. Connection strengths are almost fixed but the pairs are not perfectly stable so that the decomposition and the recomposition of the pairs occasionally occur. Furthermore, a few units do not form pairs. For such units, the connection changes drastically over time. In Fig. 4 (top), a snapshot of the connection matrix of this network structure is shown.

The structure of the second type looks almost random. Units are connected randomly, while the symmetry of the connection is very high, i.e., if w^{ij} is large then w^{ji} is also large, and vice versa. In this network, unlike the previous one, the connection strengths frequently change over time. In Fig. 4 (middle), the connection matrix of this structure is shown.

In the structure of the last type of network, units split into two groups, one composed of the units emanating a large number of connections and the other of the units having only a few connections going out of them. In Fig. 4 (bottom), the connection matrix of this structure is shown.

IV. QUANTIFICATION OF NETWORK PROPERTIES

Now, we focus our attention only on the networks observed in the desynchronized phase, because only in this phase does network structure change over time, and our interest is in dynamic networks.

In this section, we define two quantitative measures which reflect the structural and dynamical properties of each type of network observed in the desynchronized phase. Utilizing these measures, we determine the phase diagram for each network structure.

A. Activity of network

Among the three types of network observed in the desynchronized phase, only the first one has an almost static structure while the others have active connection dynamics.

As a quantity which reflects this difference, we define the activity A of the network as follows:

$$A(t,\tau_{\mathrm{m}})=\frac{1}{(N-1)^2}\frac{1}{\tau_{\mathrm{m}}}\sum_{i,j}\sum_{n=t}^{t+\tau_{\mathrm{m}}}|w_n^{ij}-w_{n-1}^{ij}|.$$

The activity A represents the average change of a connection strength over τ_{m} steps. In the above definition, to discard the transient, t is the time step when the average is started.

In Fig. 5, the activity A is plotted against a and c with a gray scale. A broadband with high activity is visible in the center of the figure. This band coincides with the area where the networks of the second and third types, mentioned in the preceding section, are observed. Outside of this band, the activity is quite low. This area coincides with the area where the network of the first type is observed.

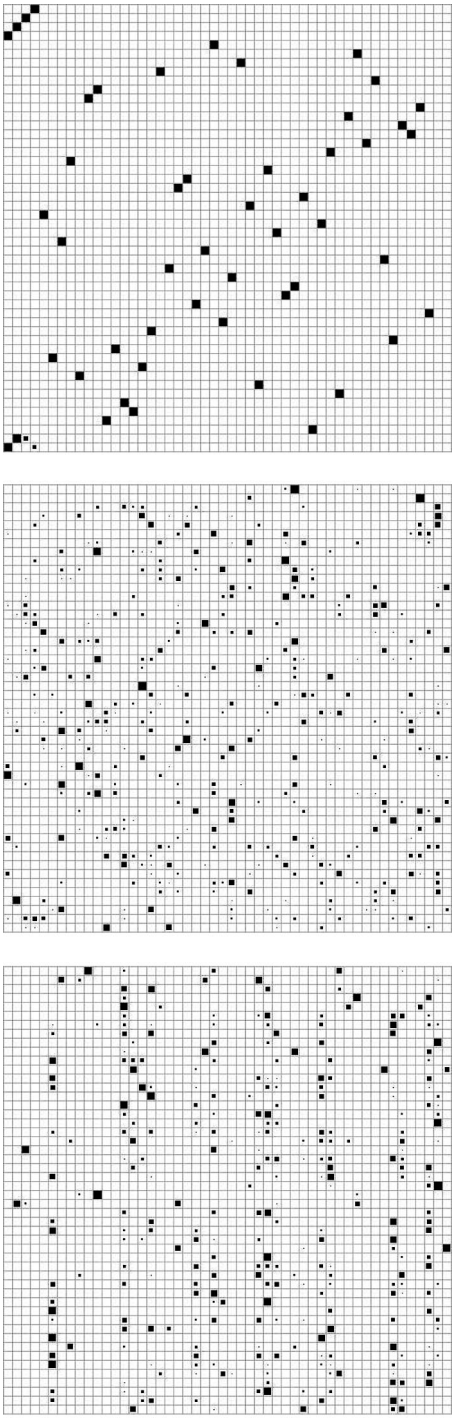

FIG. 4. Connection matrices w^{ij} of the three types of networks observed in the desynchronized phase. The scale is chosen so that the size of the corresponding square is the same as the grid size when $w^{ij}=1$. $N=50$. (Top) The first type. $a=3.97$, $c=0.2$. (Middle) The second type. $a=3.97$, $c=0.15$. (Bottom) The third type. $a=3.97$, $c=0.125$.

B. Average connection matrix

According to the value of the activity A, the desynchronized phase splits into two areas: one with a network with a static structure and the other with a dynamic structure.

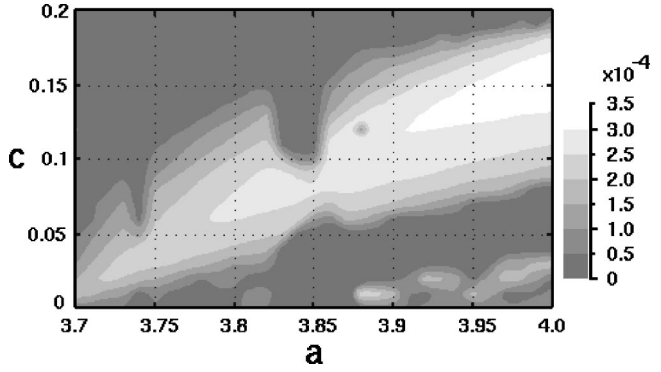

FIG. 5. Gray scale plot of the activity $A(t,\tau_m)$ of the network, obtained from the computation of the activity by changing both of the parameters by 0.01. $t=10^5$, $\tau_m=10^3$.

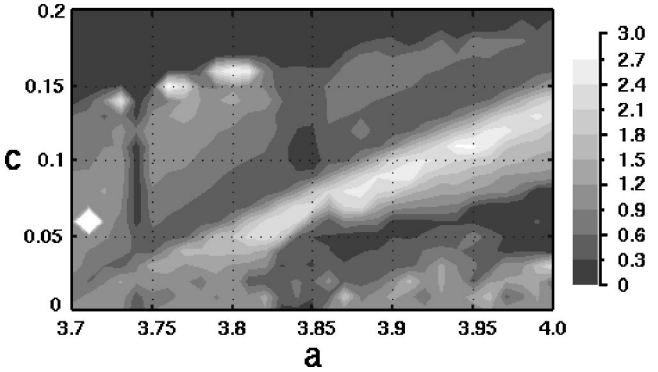

FIG. 6. Gray scale plot of the variance $(\delta W_{out})^2$ of $W_{out}{}^i(t,\tau_m)$, obtained from the computation of the variance by changing both of the parameters by 0.01 $t=10^5$, $\tau_m=10^3$.

While in the former area only one type of network structure is observed [Fig. 4 (top)], in the latter area, two types of network structure are observed [Fig. 4 (middle), (bottom)]. To quantify the difference between the latter two networks, we pay attention to the structural property of the network.

One way to do this is to consider the average connection matrix W^{ij}. W^{ij} is defined as follows:

$$W^{ij}(t,\tau_m)=\frac{1}{\tau_m}\sum_{n=t}^{t+\tau_m} w_n^{ij}.$$

W^{ij} represents the temporal average of w^{ij} over τ_m steps after the tth step. It gives a network structure averaged over time.

One can detect the existence of some stable structure by looking at the variance of W^{ij} over all pairs of i,j. If connection strengths change randomly in time, all W^{ij} will approach the same value and the variance of W^{ij} will tend to 0, as τ_t is increased. On the contrary, if the network has some temporally stable but spatially nonuniform structure, the variance will remain finite even if τ_t is increased to infinity. Since the uniform all-to-all connection structure is never realized in the desynchronized phase, the variance of W^{ij} can be considered as an index of the stability of network structure.

Recalling that in the network of the third type, strong connections tend to concentrate on a few columns [Fig. 4 (bottom)], we sum up W^{ij} over i to get the total strength of the outgoing connections of unit j, and consider the variance of this total strength over units. We define W_{out}^i as follows:

$$W_{out}^i(t,\tau_m)=\frac{1}{\tau_m}\sum_{n=t}^{t+\tau_m}\sum_{j=1}^{N} w_n^{ji}=\sum_{j=1}^{N} W^{ji}(t,\tau_m).$$

This is the temporal average of the total strength of the outgoing connections of unit i over τ_m steps after the tth step.

We calculate the variance $(\delta W_{out})^2$ of W_{out}^i over i,

$$(\delta W_{out})^2=\sum_i (W_{out}^i-\overline{W_{out}})^2$$

with

$$\overline{W_{out}}=\sum_i W_{out}{}^i/N,$$

and plot it against a and c with a gray scale. The result is shown in Fig. 6. The narrow band of the high $(\delta W_{out})^2$ is seen from the lower left to the upper right of the figure. This band coincides with the area where the network of the third type is observed. Comparing this figure with Fig. 5, it is observed that the lower half of the band of the high activity corresponds to the narrow band of the high $(\delta W_{out})^2$. The upper half of the high activity band, where $(\delta W_{out})^2$ is relatively low, coincides with the area where the network of the second type is observed.

C. Regions

Using the two quantities introduced above, we can divide the desynchronized phase into three regions, with regards to the dynamics and the stability of network structure. We call these three regions the static region, dynamic region I, and dynamic region II (Fig. 7).

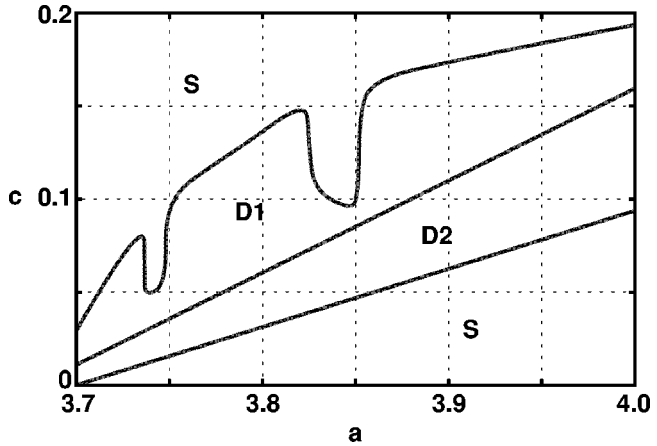

FIG. 7. Rough phase diagram with regards to the network structure, generated according to Figs. 5 and 6. Letters in the figure represent the following: S, static region; $D1$, dynamic region I; $D2$, dynamic region II.

1. Static region

This region is characterized by the low network activity *A*. In this region, most units make pairs and each unit is connected only with the partner in the pair. Although their connection strengths hardly change over time, the decomposition and the recomposition of the pairs occasionally occur. Besides those units forming pairs, there remain a few units that do not form pairs. Their connection strengths change rapidly over time.

The dynamics of units forming a pair are not synchronized, but highly correlated, while there is almost no correlation between units that belong to different pairs.

2. Dynamic region I

This region is characterized by the high activity *A* and the low $(\delta W_{\text{out}})^2$. There is no synchronization between any two units, and the correlation between units is very low for any given couple of units. Due to these disordered unit dynamics, connection strengths change intensely. Here, the network structure seems to be random.

3. Dynamic region II

This region is characterized by the high activity *A* and the high $(\delta W_{\text{out}})^2$. Similarly to the dynamic region I, there is neither synchronization nor a significant correlation between any two units. Here the network possesses a temporally stable structure, although the connection strengths change as intensely as in dynamic region I.

V. NETWORK STRUCTURE

In this section, we analyze the structure of the network quantitatively. For this purpose we map the network structure to a graph. We digitize each connection strength into a binary value. If the strength of a connection exceeds $1/(N-1)$, we assign the value "1" to that connection. Otherwise, the value "0" is assigned. The threshold value $1/(N-1)$ adopted here is the value which a connection takes when a unit connects uniformly to all the other units [18]. Hence, the connection 1 means that the correlation between the units relating to the connections is larger than the average case with a uniform connection. The set V of units and the set E of the connections with the value 1 define a graph reflecting the structure of the network in our system. Since w^{ij} is not always equal to w^{ji} in our model, the resulting graph is a directed graph.

A. Global structure

Using this graph, we compute two quantities that reflect the global feature of the network structure: the density D and the symmetry S of the graph.

The density D of a graph is defined as follows:

$$D(t)=\frac{1}{(N-1)^2}\sum_{i,j} d^{ij}(t),$$

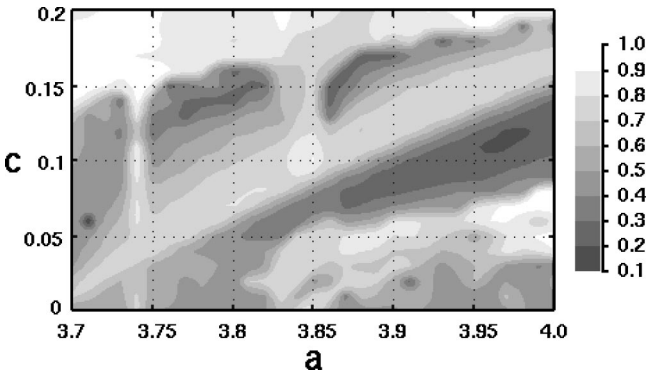

FIG. 8. Gray scale plot of the density $D(t)$ of the graph mapped from the network, obtained from the computation of the density by changing both of the parameters by 0.01. $t=10^5$.

$$d^{ij}(t)=\begin{cases} 1 & \left(w_t^{ij}\geqslant\dfrac{1}{N-1}\right) \\ 0 & \left(w_t^{ij}<\dfrac{1}{N-1}\right). \end{cases}$$

This density D represents the proportion of the actual connections in the graph to all the possible connections in the graph with N vertices at the tth step.

In Fig. 8, the density D is plotted against a and c with a gray scale. The dependence of the density D on a and c is quite similar to that of the activity A. This means that the density is high in the dynamic regions and low in the static region. The difference between the network structure in the dynamic regions I and II is not clear at this point.

The symmetry S of a graph is defined as follows:

$$S(t)=\frac{\sum_{i,j} s^{ij}(t)}{\sum_{i,j} d^{ij}(t)},$$

$$s^{ij}(t)=\begin{cases} 1 & \left(w_t^{ij}>\dfrac{1}{N-1},\ w_t^{ji}>\dfrac{1}{N-1}\right) \\ 0 & (\text{otherwise}). \end{cases}$$

The symmetry S represents the proportion of the reciprocal connections to all the connections in the graph at the tth step.

In Fig. 9, the symmetry S is plotted against a and c with a gray scale. The dependence of the symmetry S on a and c is almost opposite to that of $(\delta W_{\text{out}})^2$. The symmetry is high in the dynamic region I and low in the dynamic region II. Hence, the networks in the dynamic regions I and II have different characteristics not only in the stability of the structure but also in the structure itself.

B. Local connectivity

To reveal a more detailed network structure, we focus on indegree and outdegree of each unit in the graph. Indegree is the number of connections going out of a unit and outdegree is the number of connections arriving at a unit.

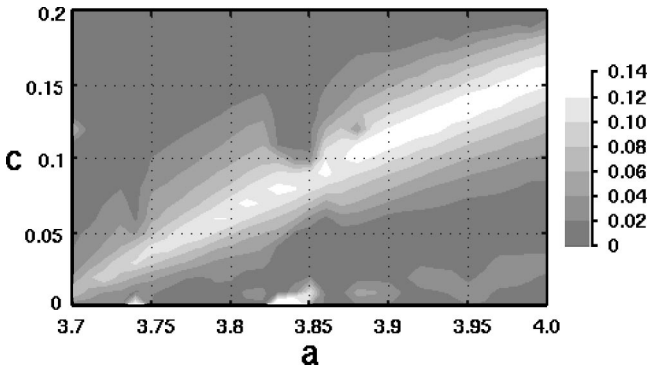

FIG. 9. Gray scale plot of the symmetry $S(t)$ of the graph mapped from the network, obtained from the computation of the symmetry by changing both of the parameters by 0.01. $t=10^5$.

In the following, we explain the structural properties of the networks observed in the three regions in the desynchronized phase according to the analysis of the distributions of indegree and outdegree.

1. Static region

As mentioned above, most units form pairs in this region. Hence the distributions for both of the indegree and the outdegree are mostly concentrated on the value 1, and have a very sharp peak at this value.

2. Dynamic region I

In Fig. 10 (top), the distributions of the indegree and outdegree of the network observed in the dynamic region I are shown. The peaks of both distributions are almost at the same position, while the distribution of the indegree has a smaller variance and a higher peak than the outdegree distribution. This difference is due to the normalization of the total incoming connection strength. Both distributions are well approximated by the normal distribution (not shown), which implies that the units are randomly connected. Note that these distributions are calculated from snapshots of the connection matrices. Hence, they carry no information about the temporal aspect of the network structure.

To reveal the temporal properties, we count the indegree and the outdegree of one arbitrarily chosen unit for a long time and compute their distributions. The result is shown in Fig. 10 (bottom). Comparing it with the previous figure, one can easily see that these distributions take almost the same shape, which implies that the network structure changes almost randomly.

3. Dynamic region II

In Fig. 11, the distributions of the indegree and the outdegree of the network observed in the dynamic region II are shown.

Though the indegree distribution is similar to that in the dynamic region I, their outdegree distributions are quite different. The outdegree distribution in the dynamic region II is given by the superposition of two components: one ranging from 0 to about 16, showing exponential decay from the

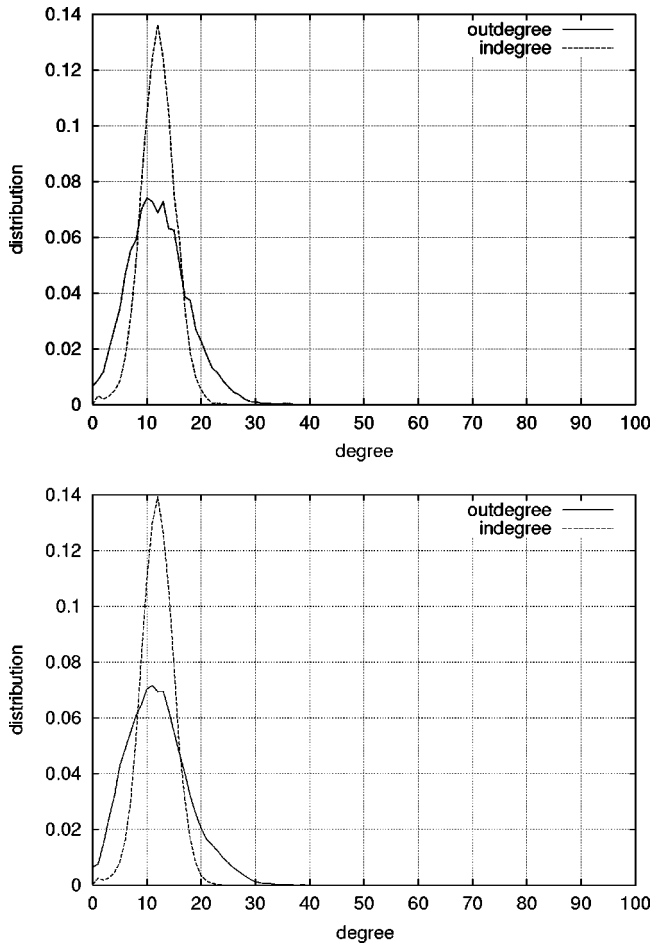

FIG. 10. Distributions of the indegree and outdegree of the graph. Solid line: outdegree. Broken line: indegree. $N=100$, $a=3.97$, $c=0.15$. (Top) Distributions of the indegree and outdegree of the units in the graph mapped from the networks at the 10^6th step of 100 trials with different initial conditions. (Bottom) Distributions of the indegree and outdegree of an arbitrarily chosen unit in the graph mapped from the networks at the (1.0×10^6)th to the (2.0×10^6)th step.

peak at 0, and the other from about 16 to about 68, which has the shape of a normal distribution with its peak at about 40.

This implies that units are separated into two groups. The proportions of the number of the units in the group with the lower outdegree and that with the higher outdegree to the whole system are 0.82 and 0.18, respectively.

As mentioned above, these distributions tell nothing about the temporal change of the network structure. Hence, it is not clear whether the separation of units is stable over time (i.e., the groups do not exchange their members with each other) or not. To answer this question, we study the evolution of W^i_{out}.

In Fig. 12, the time series of W^i_{out} is plotted for all i at every 10^4 steps, where the units whose W^i_{out} at the 10^7th step exceed 2 are plotted with red lines and the remaining units are plotted with green lines. Though the assignment of the color to each unit is determined only by the value of W_{out} at the 10^7th step, almost all of the units in the group with the

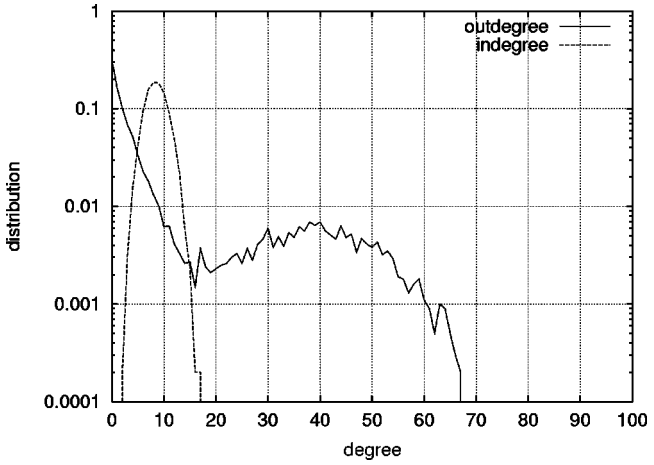

FIG. 11. Distributions of the indegree and outdegree of the units in the graph mapped from the networks at the 10^6th step of 100 trials with different initial conditions. Note the logarithmic scale used in the vertical axis. $N=100$, $a=3.97$, $c=0.125$.

higher outdegree are plotted with red lines over much longer time steps. This means that most of the units with higher $W^i_{\rm out}$ values at the early stage of the separation still have higher $W^i_{\rm out}$ values. Hence it is concluded that the separation of units is highly stable.

Next we confirm the separation of units more quantitatively by defining an appropriate measure for the separation. Here we define an autocorrelation function relating to the separation of units in the following way.

First, we define a binary variable b^i_n, which takes 1 if the unit i belongs to the group with higher outdegree, and -1 otherwise, i.e.,

$$b^i_n=\begin{cases}1 & \left(\sum_{j=1}^{N} w^{ji}_n \geqslant 1.0\right)\\ -1 & \left(\sum_{j=1}^{N} w^{ji}_n < 1.0\right).\end{cases}$$

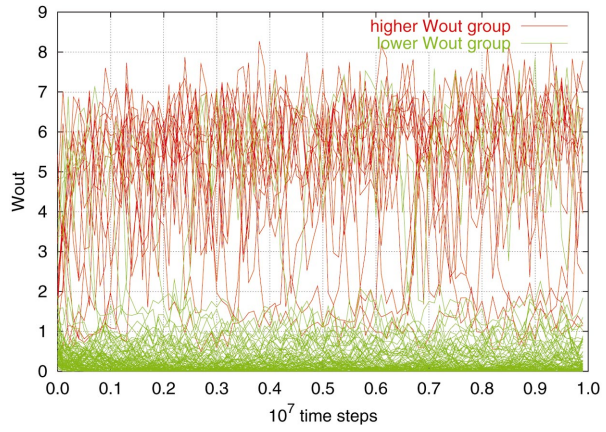

FIG. 12. (Color) Temporal evolution of $W^i_{\rm out}(t,\tau_{\rm m})$. Each line represents the time series of $W^i_{\rm out}$. The time series for all i are superimposed. The red lines correspond to the units whose $W^i_{\rm out}$ at the 10^7th step exceed 2 and the green lines to the rest of the units. $\tau_{\rm m}=10^5$, $N=100$, $a=3.97$, $c=0.125$.

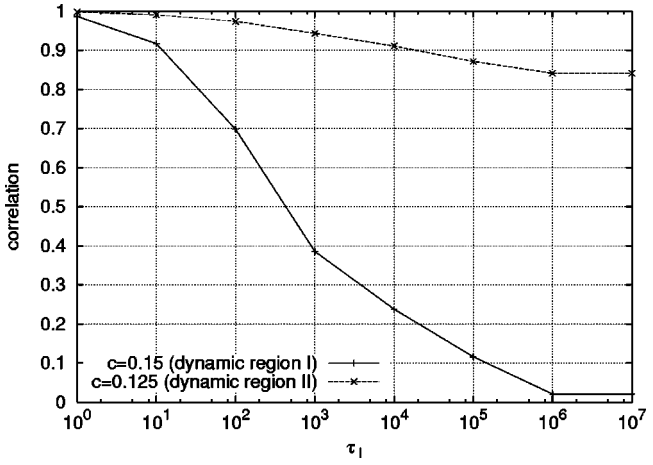

FIG. 13. Plot of $C_{\rm sep}(t,\tau_{\rm m},\tau_{\rm l})$ against $\tau_{\rm l}$. Note the logarithmic scale used in the horizontal axis. $t=10^6$, $\tau_{\rm m}=10^4$. $N=100$. Solid line: dynamic region I ($a=3.97$, $c=0.15$). Broken line: dynamic region II ($a=3.97$, $c=0.125$).

The threshold value 1.0 used here is the average of the total outgoing connection strength of a unit. Then, we define the autocorrelation function $C_{\rm sep}$ between b^i_n and $b^i_{n+\tau_{\rm l}}$ as follows:

$$C_{\rm sep}(t,\tau_{\rm m},\tau_{\rm l})=\frac{1}{N}\sum_{i=1}^{N} C^i_{sep}(t,\tau_{\rm m},\tau_{\rm l}),$$

$$C^i_{\rm sep}(t,\tau_{\rm m},\tau_{\rm l})=\frac{\sum_{n=t}^{t+\tau_{\rm m}} b^i_n b^i_{n+\tau_{\rm l}}}{\sum_{n=t}^{t+\tau_{\rm m}} b^{i\,2}_n}=\frac{1}{\tau_{\rm m}}\sum_{n=t}^{t+\tau_{\rm m}} b^i_n b^i_{n+\tau_{\rm l}}.$$

We can measure the stability of the separation by looking at how $C_{\rm sep}$ decays as $\tau_{\rm l}$ gets larger.

The plot of $C_{\rm sep}$ against $\tau_{\rm l}$ is shown in Fig. 13. The dependence of $C_{\rm sep}$ on $\tau_{\rm l}$ in the dynamic region I and the dynamic region II is drawn with the solid and the broken lines, respectively. In the dynamic region II, the correlation decays very slowly and it remains very strong, namely, 0.84, even for the lag of 10^7 steps, while in the dynamic region I, the correlation decays to almost zero within 10^6 steps. Hence, the separation of the units is highly stable in the dynamic region II, while the separation is unstable, or never occurs, in the dynamic region I.

C. Temporal evolution of the network structure

In this section, we study the time course of the formation of the network structure in more detail. As a simple way to illustrate network structure, we adopt the following method. First, after the temporal evolution for certain steps, a graph is generated with the method introduced above. Then, we compute the indegree and the outdegree of each unit from the graph, and calculate their average separately for each unit over a certain period of time steps. These averages of indegree and outdegree are plotted on a two-dimensional plane

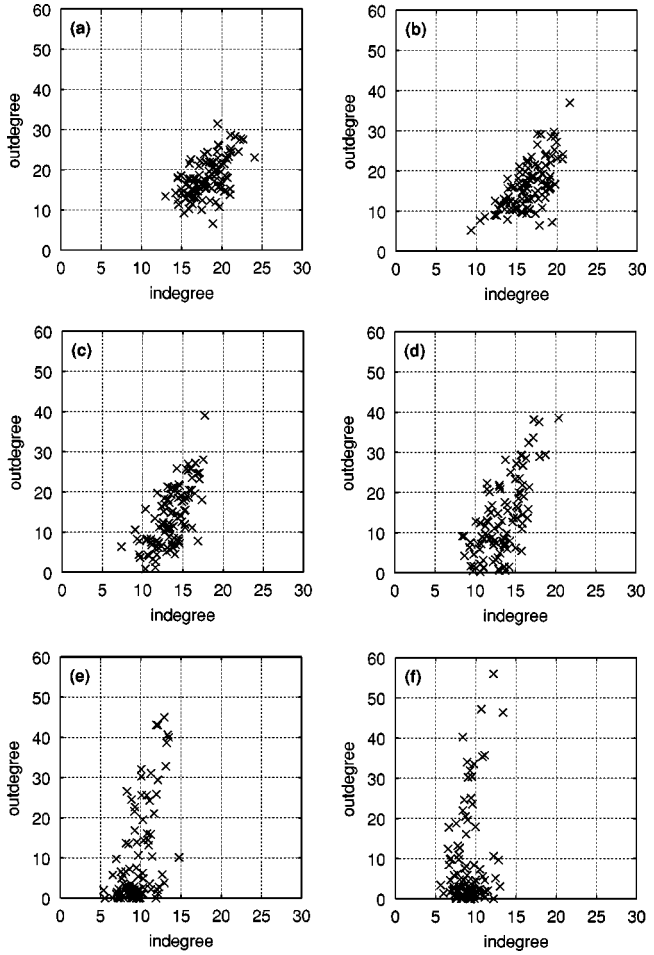

FIG. 14. Degree scattergrams of the network in the dynamic region II. $N=50$, $a=3.97$, $c=0.125$. (a) From the 0th to the 1000th step. (b) From the 1000th to the 2000th step. (c) From the 5000th to the 6000th step. (d) From the 10 000th to the 11 000th step. (e) From the 50 000th to the 51 000th step. (f) From the 100 000th to the 101 000th step.

with the abscissa for indegree and the ordinate for outdegree. We call this type of plot a ''degree scattergram'' here. We study the temporal change of the network structure from the degree scattergrams for different time spans.

In Fig. 14, the degree scattergrams of the network in the dynamic region II are plotted for different time spans. In the initial state, all units have the same indegree and outdegree, namely, $N-1$. Right after the start of the simulation, indegree and outdegree rapidly decrease. In the plot over 0–1000 steps [Fig. 14(a)], indegree and outdegree for each unit scatter around 20. The average of both degrees keeps decreasing slowly, while the variance of the outdegree gets larger and larger [Figs. 14(b) and 14(c).] The distribution of outdegree still gets broader after the 10 000th step, while the average and the variance of the indegree get smaller [Figs. 14(d)–14(f)]. Throughout this process, there exists strong positive correlation between indegree and outdegree.

From about the 50 000th step, units start to split into two groups [Figs. 14(e) and 14(f).]. The separation gets clearer with time. In Fig. 15, the degree scattergram for the period of 1000 steps starting from the 10^6th step is shown. The separation of the units is clearly seen.

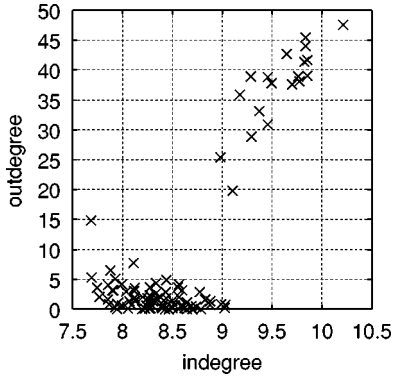

FIG. 15. Degree scattergram of the network in the dynamic region II for the period of 1000 steps starting from the 10^6th step. Note that the scales in both axes are different from those in Fig. 14. $N=50$, $a=3.97$, $c=0.125$.

Next, we show the degree scattergrams of the network in the dynamic region I in Fig. 16. As in the dynamic region II, indegree and outdegree slowly decrease [Figs. 16(a)–16(c)]. However, the distribution of the points is sharper than in the dynamic region II. After slowly decreasing for a while [Figs. 16(b) and 16(c)], the degrees hardly change their distributions after the 10 000th step [Figs. 16(d)–16(f)].

The positive correlation between indegree and outdegree is observed again, though it is much weaker than in the dynamic region I. The existence of such a correlation in this region is natural, considering the high symmetry of the network in this region. Still, the deviation from the perfect symmetry, i.e., the deviation of the points from the line where outdegree is equal to indegree drawn in Fig. 16(f), is more interesting. The units with larger outdegrees tend to take a much larger outdegree, which suggests the existence of a positive feedback mechanism to amplify the deviation of outdegree from the average.

VI. MECHANISM OF STRUCTURE FORMATION

In this section we reveal the relationship between unit dynamics and the formation of the network structure.

In this section, we fix the parameter a to 3.97 and consider the dependence of the network structure only on the parameter c, for simplicity. Needless to say, the results drawn are applicable to the case with the other values of a.

In Fig. 17, the dependence of the activity A of the network and $(\delta W_{\mathrm{out}})^2$ on c is shown for $a=3.97$. From these figures, it can be seen that, for $a=3.97$, the static region lies in the intervals $0<c\lesssim 0.075$ and $0.19\lesssim c$, the dynamic region I in the interval $0.145\lesssim c\lesssim 0.19$, and the dynamic region II in the interval $0.075\lesssim c\lesssim 0.145$.

A. Boundary between the static and the dynamic regions

First, we study how the boundary between the static and the dynamic regions is determined in relation to the unit dynamics.

As mentioned above, most units form pairs in the static region. The units forming a pair have connections only be-

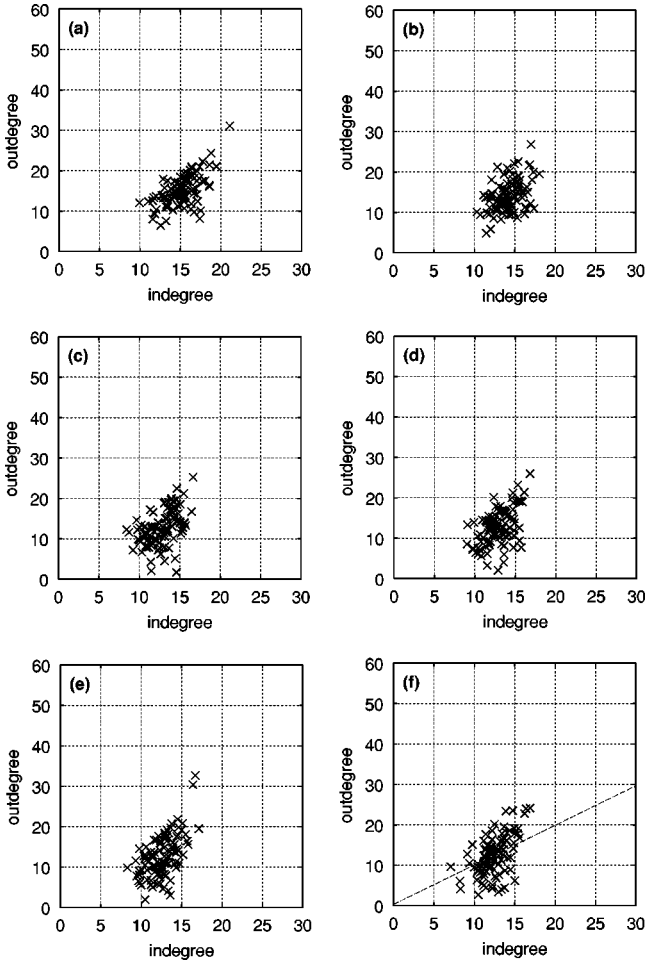

FIG. 16. Degree scattergrams of the network in the dynamic region I. $N=50$, $a=3.97$, $c=0.15$. (a) From the 0th to the 1000th step. (b) From the 1000th to the 2000th step. (c) From the 5000th to the 6000th step. (d) From the 10 000th to the 11 000th step. (e) From the 50 000th to the 51 000th step. (f) From the 100 000th to the 101 000th step. The broken line represents the line where outdegree is equal to indegree.

tween each other. Accordingly an interaction between different pairs hardly exists. Hence, we can roughly grasp the behavior of the whole system in the static region by looking only at the dynamics of a single pair. The dynamics of a single pair obeys the following equations:

$$x^0_{n+1}=f((1-c)x^0_n+cx^1_n),$$

$$x^1_{n+1}=f((1-c)x^1_n+cx^0_n),$$

where x^0_n and x^1_n represent the state variables of the units forming a pair.

In Fig. 18, the bifurcation diagram of the dynamics of a pair against c for $a=3.97$ is shown. The difference between x^0_n and x^1_n is plotted against c within the interval $0<c<0.3$. For $c\gtrsim 0.223$, the difference is 0, which means that the dynamics of the units are synchronized. This range of c corresponds to the ordered phase. Needless to say, the interval $0<c\lesssim 0.223$ corresponds to the desynchronized phase.

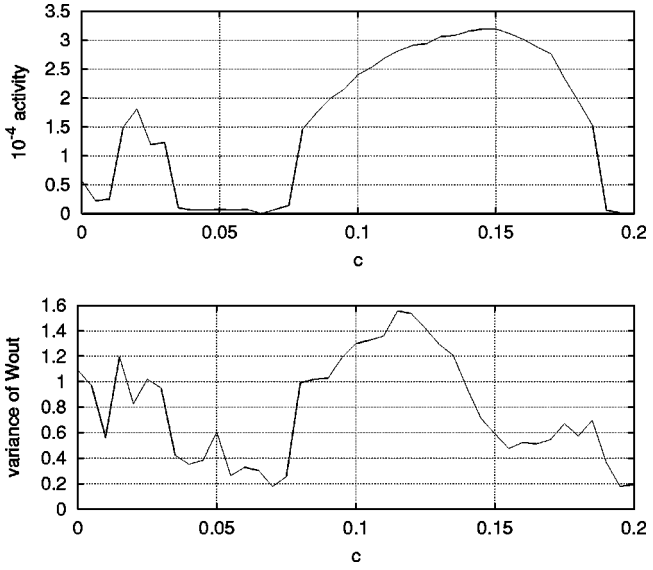

FIG. 17. Dependence of the activity $A(t,\tau_m)$ of the network (top) and the variance of $W^i_{out}(t,\tau_m)$ (bottom) on c. $t=10^5$, $\tau_m=10^3$, $a=3.97$.

In the intervals $0<c\lesssim 0.075$ and $0.185\lesssim c\lesssim 0.223$, which lie within the desynchronized phase, the difference between the two units is not zero but changes chaotically over time. However, it stays close to zero over a large proportion of time steps, as can be seen from the dense points around zero in Fig. 18. During the time steps satisfying $x^0_n\approx x^1_n$, the coupling between the two units is amplified, which overcomes the depression of the coupling during the time steps where the difference is large. Hence the pairing structure is stable here. The static region coincides with these intervals.

On the other hand, in the interval $0.075\lesssim c\lesssim 0.185$, the difference takes much larger values. In particular, in the interval $0.13\lesssim c\lesssim 0.18$, it shows period-2 oscillation. This is due to the antiphase oscillation of the two units. Such an antiphase oscillation, however, is observed only when we isolate a single pair from the system. In the original system where the connection strengths can vary, if such an antiphase

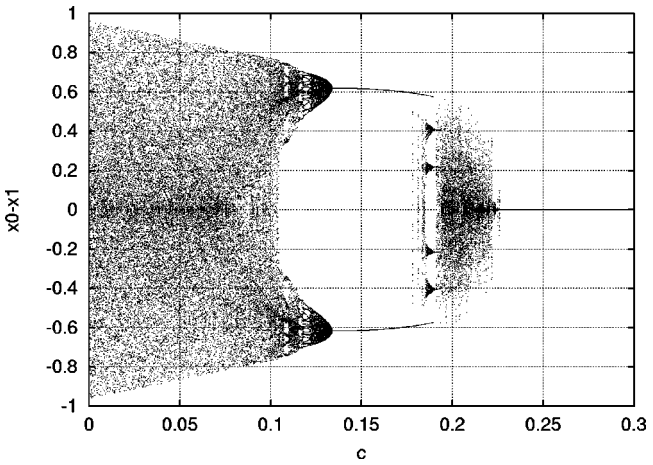

FIG. 18. Bifurcation diagram of the dynamics of a pair for $a=3.97$. The difference between x^0_n and x^1_n is plotted against c.

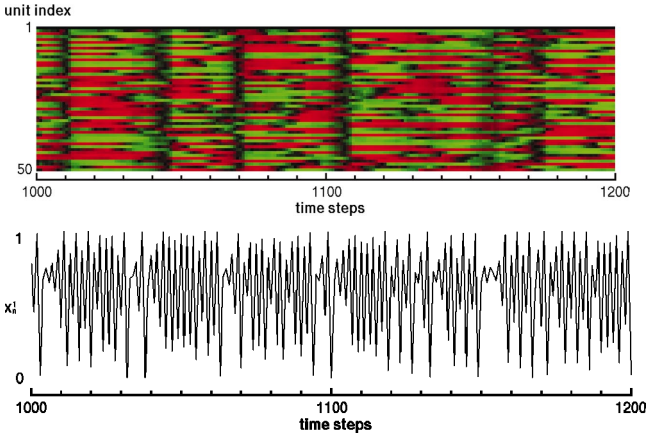

FIG. 19. (Color) (Top) Temporal change of the correlation between an arbitrarily chosen unit (unit 1) and the other units in the system. The correlations between units' dynamics in the past ten steps are plotted in a color scale at every step. Green and red colors correspond to positive and negative correlations, respectively, while the brightness of the colors shows the strength of the correlation. $N=50$, $a=3.97$, $c=0.15$. (Bottom) Time series of the dynamics of the chosen unit (unit 1 in the top figure).

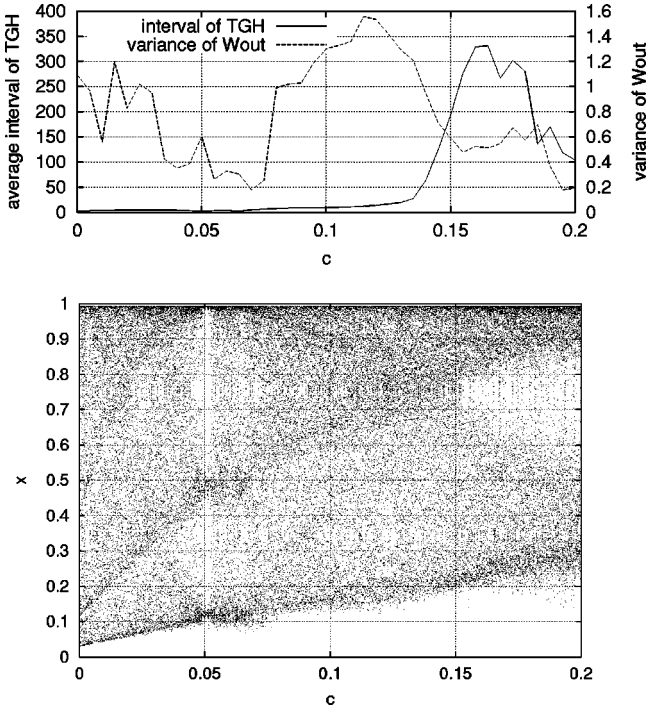

FIG. 20. (Top) The dependence of the average interval of TGH and $(\delta W_{\mathrm{out}})^2$ on c. (Bottom) Bifurcation diagram of the dynamics of a unit in the ordinary GCM. (All connection strengths are fixed and identical.)

oscillation occurred, the connection between the units forming the pair would be weakened rapidly, which results in the decomposition of the pair. Hence, in this interval, pairs are unstable. The dynamic regions correspond to this intervals.

B. Boundary between the dynamic regions I and II

Next, we study the boundary between the dynamic region I and the dynamic region II.

In the dynamic regions, each unit is connected to many other units in a complex manner. Therefore, it is impossible to estimate the whole system's behavior only from the dynamics of some particular units. Here, we trace the dynamics of an arbitrarily chosen unit, compute the correlation between the chosen unit and the other units' dynamics over a short time period, namely ten steps, at every step, and plot their temporal change.

In Fig. 19, the dynamics of an arbitrarily chosen unit and its correlations with the other units in the dynamic region I are shown. The correlations are plotted in a color scale, where green or red represents a positive or negative correlation, respectively, and the brightness of the color indicates the magnitude of the correlation.

The temporal change in the correlations has the following characteristics.

(1) A strong positive (or negative) correlation lasts for a certain number of steps, followed by a short period with a weak correlation.

(2) After this period, the sign of the correlation changes for most cases.

The simultaneous appearance of the short period with a weak correlation for all units is accompanied by the approach of the units' state variables to the (unstable) fixed point of the logistic map $(0.748\ldots)$. Note that the dynamics of the logistic map here are two-band motions, i.e., the unit takes values larger or smaller than the fixed point alternately. According to the phase of this oscillation, units are naturally separated into two groups: when the units of one group take high values, the others take low values, and vice versa. This separation, however, is not stable because each unit sometimes fails to cross over the fixed point, which turns the phase to the opposite.

The period with weak a correlation is nothing but the movement of a unit from one group to the other. As a unit switches to the other group of the opposite phase (i.e., from high-low-high-$\cdots$ to low-high-low-$\cdots$), the sign of the correlation changes [19].

We call this movement of a unit from one group to the other a ''trans-group hopping'' (TGH). TGH is closely related to the temporal change in correlations between units. The dynamics of TGH are expected to have a strong influence on the formation of network structures.

To investigate the dynamic characteristics of TGH, we focus on the average interval between two successive TGHs. The intervals are measured in the ordinary GCM, where all connection strengths are fixed and identical, because we now want to obtain the expected value of the interval of TGH in the network with a certain structure.

In Fig. 20 (top), the dependence of the average interval of TGH on c is plotted, as well as the dependence of $(\delta W_{\mathrm{out}})^2$ on c. The average interval of TGH shows a rapid increase around $c=0.15$, where $(\delta W_{\mathrm{out}})^2$ shows a rapid decrease. This value of c is nothing but the transition point from the dynamic region II to the dynamic region I. This suggests that the change in the average interval of TGH leads to the

change in the network structure from the region I to II, which will be discussed below.

To see what change in unit dynamics causes the sudden change in the TGH frequency, we plot the bifurcation diagram of a unit in the ordinary GCM, which is used to calculate the average TGH interval, against c for $a=3.97$ in Fig. 20 (bottom).

For $c \gtrsim 0.15$, the unit shows a two-band chaos and hardly takes a value around the fixed point. Hence, it can be said that TGH hardly occurs in the two-band chaos state. In fact, the average interval of TGH is very long here. Around $c=0.15$, band merging occurs and the unit shows a single-band chaos for $c \lesssim 0.15$, and the average interval of TGH rapidly decreases. Therefore, it can be concluded that the sudden change of the TGH frequency is caused by the bifurcation of the unit dynamics from the two-band chaos to the single-band chaos.

C. Feedback between dynamics and structure

In this section, we study the relationship between unit dynamics and the formation of network structure, focusing on the relationship between TGH and the structure formation in the dynamic region II.

Here we compute the average interval between two succeeding TGHs of each unit in the network. The TGH interval of each unit is measured with the following method. After discarding the transient over the first τ_f steps, we fix the connection strength, allowing only for the evolution of the state variables. Then we measure the TGH intervals of each unit for a certain time period and compute the average separately for each unit over the period.

We plot the obtained average interval against W^i_{out} for each unit to investigate the influence of the network structure on unit dynamics. The plots for six different values of τ_f are shown in Fig. 21. Initially, the intervals are almost the same for all units [Fig. 21(a)]. Then, the intervals start to differ by units [Figs. 21(b)–21(d)], where a positive correlation between W^i_{out} and the intervals is observed. A unit with a larger W^i_{out} value has a smaller rate of TGH. At later times, the correlation gets weaker [Figs. 21(e) and 21(f)]. Note that the period when the correlation between W^i_{out} and the TGH intervals is strongest coincides with the period when the correlation between indegree and outdegree is strongest, namely, from the 5000th step to the 10 000th step [Figs. 14(c) and 14(d)].

This observation shows how network structures influence the frequency of TGH. Next, we consider the opposite influence, i.e., the influence of unit dynamics on the formation of the network structure. Here we measure the correlation between units, instead of the network structure, since the connection between units with a strong correlation is amplified in our model.

We measure the average correlation C^i of unit i with all the other units' dynamics, defined as follows:

$$C^i = \frac{1}{N-1} \sum_{j \neq i} \frac{|\langle x^i_n x^j_n \rangle - \langle x^i_n \rangle \langle x^j_n \rangle|}{\sqrt{\langle x^{i\,2}_n \rangle - \langle x^i_n \rangle^2} \sqrt{\langle x^{j\,2}_n \rangle - \langle x^j_n \rangle^2}}.$$

C^i is computed by fixing the connection as mentioned above.

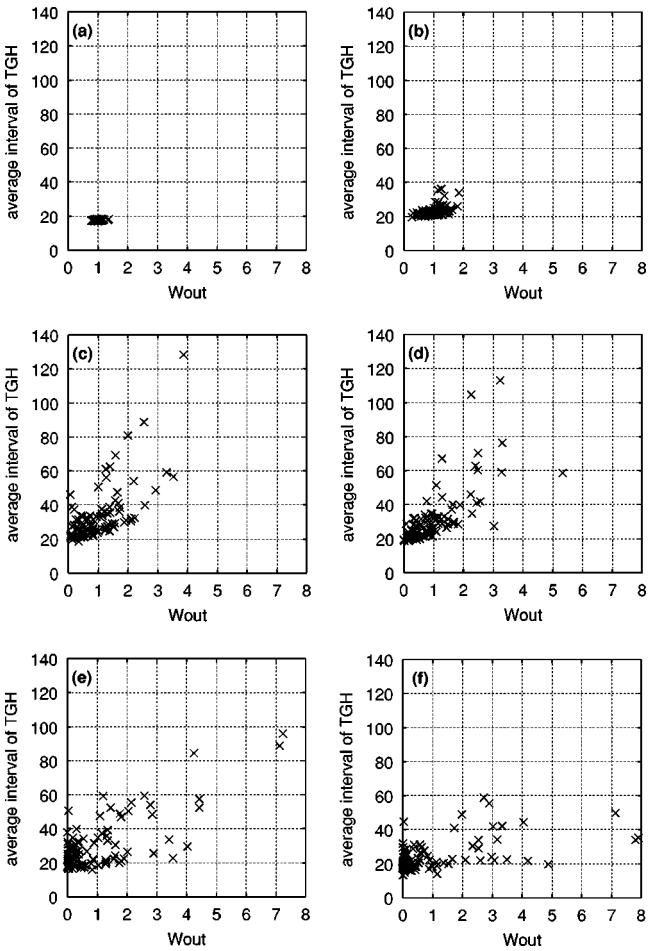

FIG. 21. Plot of the average intervals of TGH against W^i_{out}. Each point in a figure corresponds to each unit. $N=50$, $a=3.97$, $c=0.125$. (a) $\tau_f=100$. (b) $\tau_f=1000$. (c) $\tau_f=5000$. (d) $\tau_f=10\,000$. (e) $\tau_f=50\,000$. (f) $\tau_f=100\,000$.

In Fig. 22, the average correlation C^i is plotted against the average interval of TGH for $\tau_f=10\,000$. There is a clear relationship between C^i and the TGH interval. A unit with a

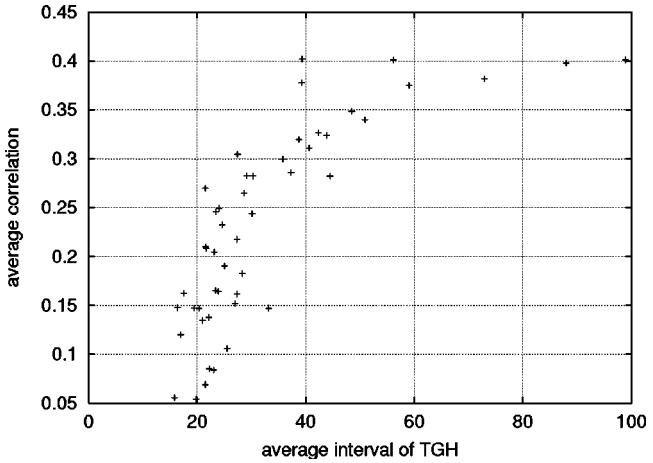

FIG. 22. Plot of the average correlation C^i against the average interval of TGH. Each point in the figure corresponds to each unit. $\tau_f=10^4$, $N=50$, $a=3.97$, $c=0.125$.

longer TGH interval has a stronger average correlation. Because C^i gives a measure of the degree of the increase in connections from a unit, this result means that a unit with a longer TGH interval is more likely to strengthen its connections.

Now, we have confirmed the bidirectional influence between unit dynamics and the formation of the network structure. A unit with a smaller TGH rate grows its connections more rapidly, and a unit with stronger connections decreases the rate of TGH. This mutual reinforcement amplifies the difference among the connection strengths of units. One consequence of this amplification is the separation of connections in the dynamic region II.

In the dynamic region I, the correlation among units is generally strong, as is confirmed by the long TGH interval [Fig. 20 (top)]. Hence, the units are kept from separating into groups. The consequence of the amplification is seen only in the deviation of the indegree and outdegree from perfect symmetry.

In the dynamic region II, the correlation among units is weak due to the frequent TGH. Therefore, the amplification of the difference among the connection strengths of units works effectively, which results in the separation of units into the two groups. Now the origin of this separation is understood as the positive feedback process between unit dynamics and network structure.

VII. SUMMARY AND DISCUSSION

We studied basic properties of coupled maps with variable connection strengths, by adopting a version of globally coupled maps (GCM's) as our model. Differently from the ordinary GCM, our model does not have the partially ordered phase in the parameter space. This is due to the stabilization of clusters by the change of connections. In our model, once a cluster is formed, its interaction with the rest of the system tends to vanish because the connections between units within and out of the cluster are weakened. This stabilizes the clusters.

In the coherent and the ordered phase, connection strengths are fixed asymptotically because of the synchronization between units. In the desynchronized phase, there is no synchronization between any pair of units, and the connection strength can change in time. In spite of chaotic dynamics of units, however, connection matrix has a certain structure.

We classified the network structure into three types, and partitioned the desynchronized phase into three regions, i.e., the static region, the dynamic region I, and the dynamic region II, corresponding to each network structure. In the static region, most of the units form a pair, and a unit in a pair is connected only with its partner. Change of connection strengths is slight and the decomposition and recomposition of pairs hardly occur. In the dynamic region I, units are connected in a random manner and temporal change of connections is large. In the dynamic region II, units split into two groups: one group composed of units with a large number of outgoing connections and the other units with a few outgoing connections. Temporal change of connections is large as in the dynamic region I but the separation of units is stable over time.

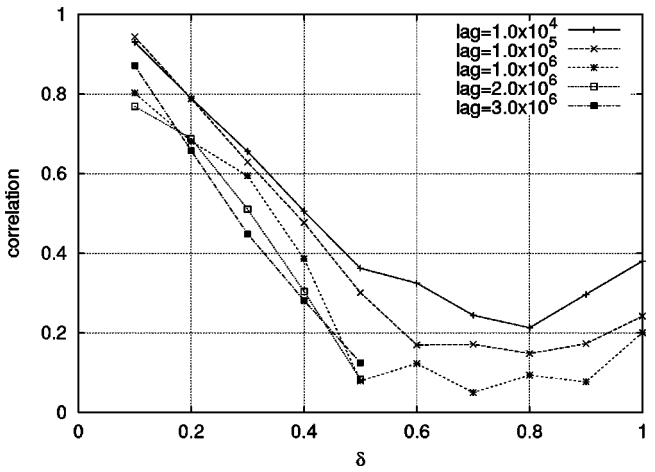

FIG. 23. Plots of $C_{\mathrm{sep}}(t,\tau_{\mathrm{m}},\tau_{\mathrm{l}})$ against δ for different values of τ_{l}. $t=10^6$, $\tau_{\mathrm{m}}=10^4$. $N=100$.

Boundaries between the regions are related to the change in the type of unit dynamics. Across the boundary between the static region and the dynamic regions, the stability of antiphase oscillating dynamics changes. Switching of the phase of two-band oscillations appears in the dynamic regions, leading to trans-group hopping (TGH). The boundary between the dynamic regions I and II is given by the change in the frequency of TGH.

The mechanism of the structure formation in the dynamic regions is clarified as a mutual reinforcement between the unit dynamics and the connection dynamics. Within the unit dynamics, correlations with other units start to differ by units, leading to the difference in connection strengths. In turn, this difference in connection strengths leads to the difference in TGH frequency among units, which leads to the difference in correlations. Hence, the differences among connection strengths are amplified, which results in the separation of units in the dynamic region II.

In this mechanism of structure formation, it is essential that the unit dynamics have the two states characterized by the phase of oscillation. Here, the rate of the change between the states, rather than the values of the unit variables, is important for the structure formation. We expect that this observation can be applied to any network system with unit dynamics. Indeed, a network of units with excitable states and variable connection strength shows unit separation of the same kind as in the present model, in spite of the significant difference in the unit dynamics. In our model (and this network of excitable states), unit dynamics take only two possible states that are clearly distinguished. What kind of network structure is formed in the system composed of units with multiple states is an interesting question.

Throughout this paper, we have fixed the value of δ to 0.1. Since δ represents the degree of plasticity of the connection, it is assumed that the stability of the separation depends on the value of δ. In Fig. 23, C_{sep} is plotted against δ for different τ_{l}. For δ larger than 0.5, C_{sep} decays to almost zero, while for δ smaller than 0.5, a finite value of C_{sep}

remains for significantly large τ_1, namely, 10^6 steps [20]. This result means that a dynamic network with a highly plastic connection change is unable to preserve structural information.

The separation of units into the two groups means the appearance of units with much more influence on the dynamics of other units. This can be regarded as the spontaneous emergence of the ''controlling part'' within the system. Such emergence may be related to the origins of hierarchy, division of labor, and leadership in some living and social systems. Indeed, because of the simplicity of the model and the universality among globally coupled maps, it is expected that such an influential group of units generally emerges in networks whose connections change in a manner governed by the relationships between its dynamic elements.

As discussed in Ref. [15], one example of such networks is the neural network of newborn organisms. Here we quote another example, i.e., networks of communication. With the growth of mass communication and the Internet, it is getting easier to broadcast information, while the cost of filtering of significant information from the large amount of useless information is getting larger and larger. Since, in such situations, one cannot examine all the information available, it becomes necessary to focus attention on a certain portion. This is the situation where our model seems well suited. Here, the emergence of the influential group may correspond to the emergence of opinion leaders. Such a correspondence seems to suggest that leadership in a group can emerge through the dynamics of a relationship among the members, even if there is no difference among their personalities.

Finally, we note that the separation of units into the two groups leads to the robustness of the network against random failures. In Ref. [16], Albert *et al.* showed that scale-free networks are highly tolerant against random failures, and discussed that this robustness of scale-free networks is rooted in their extremely inhomogeneous connectivity distribution, where the majority of nodes have only a few links. The same type of inhomogeneity of connectivity is also observed in our system, implying such a robustness against random failures. Albert *et al.* used the model of preferential attachment to generate scale-free networks. In their model, a new edge is connected preferentially to the units with high connectivity. Though we did not explicitly adopt this kind of rule for connection change in our model, a connection change of a similar nature spontaneously emerged from the interplay between unit and connection dynamics. The feedback mechanism of the separation of units in our model may supply the dynamical basis for the preferential attachment in dynamic growing networks [21].

This work was partially supported by the Special Postdoctoral Researchers Program of RIKEN.

[1] H. Jeong, B. Tombor, R. Albert, Z.N. Oltvai, and A.-L. Barabási, Nature (London) **407**, 651 (2000); A. Maslov and K. Sneppen, Science **296**, 910 (2002); E. Ravasz, A.L. Somera, D.A. Mongru, Z.N. Oltvai, and A.-L. Barabási, *ibid.* **297**, 1551 (2002).

[2] D.G. Albertson and J.N. Thomson, Philos. Trans. R. Soc. London, Ser. B **275**, 299 (1976); J.G. White *et al.*, *ibid.* **314**, 1 (1976).

[3] J.H. Brown, T.G. Whitham, S.K.M. Ernest, and C.A. Gehring, Science **293**, 643 (2001).

[4] M. Girvan and M.E.J. Newman, Proc. Natl. Acad. Sci. U.S.A. **99**, 7821 (2002).

[5] F. Liljeros, C.R. Edling, L.A.N. Amaral, H.E. Stanley, and Y. Åberg, Nature (London) **411**, 907 (2001).

[6] R. Albert, H. Jeong, and A.-L. Barabási, Nature (London) **401**, 130 (1999).

[7] D.J. Watts, *Small World* (Princeton University Press, Princeton, NJ, 1999); A.-L. Barabási, *Linked: The New Science of Networks* (Perseus Publishing, Cambridge, MA, 2002); L.A.N. Amaral, A. Scala, M. Barthélémy, and H.E. Stanley, Proc. Natl. Acad. Sci. U.S.A. **97**, 11 149 (2000); R. Milo, S. Shen-Orr, S. Itzkovitz, N. Kashtan, D. Chklovskii, and U. Alon, Science **298**, 824 (2002).

[8] D.J. Watts and S.H. Strogatz, Nature (London) **393**, 440 (1998).

[9] A.-L. Barabási and R. Albert, Science **286**, 509 (1999).

[10] K. Kaneko, Physica D **75**, 55 (1994); J. Ito and K. Kaneko, Neural Networks **13**, 275 (2000).

[11] K. Kaneko, Physica D **34**, 1 (1989).

[12] K. Kaneko, Physica D **41**, 137 (1990).

[13] K. Kaneko and I. Tsuda, *Complex Systems: Chaos and Beyond* (Springer-Verlag, Berlin, 2000); K. Kaneko, Phys. Rev. Lett. **78**, 2736 (1997); Physica D **124**, 322 (1998).

[14] S.C. Manrubia and A.S. Mikhailov, Phys. Rev. E **60**, 1579 (1999).

[15] J. Ito and K. Kaneko, Phys. Rev. Lett. **88**, 028701 (2002).

[16] R. Albert, N. Jeong, and A.-L. Barabási, Nature (London) **409**, 542 (2001).

[17] It is reported that the disappearance of the partially ordered phase is also observed in a GCM on a random network with fixed connection strengths. See Ref. [14].

[18] As long as the threshold is around this value, the same structure of graph is obtained.

[19] When the chosen unit for the plot of Fig. 19 switches from one group to the other, all the signs of correlations change simultaneously, while the change for a single pair is observed for a switch of any other unit.

[20] For very small values of δ, it is difficult to detect the occurrence of the separation with numerical simulation, since the separation requires many more steps as δ becomes smaller. However, at least for numerically amenable values of δ, lower bound of δ for the occurrence of the separation has not been detected.

[21] Relating to a model of a dynamic growing network, see P. Gong and C. van Leeuwen, Physica A **321**, 679 (2003).